Proceedings of the Institute of Acoustics

MODELING SWATH BATHYMETRY/SIDESCAN SONAR IMAGE RETURNS

J.W. Caruthers(1) & J.C. Novarini(2)

(1) Naval Research Laboratory, Stennis Space Center, MS 39529
(2) Planning Systems, Inc., 115 Christian Lane, Slidell, LA 70458

1. INTRODUCTION

There are several systems in current use that collect bathymetric data across a swath under the ship, and simultaneously collect backscattering data similar to sidescan images. The bathymetric data allows for low spatial frequency descriptions of the bottom geomorphology and we argue here that the backscattering data can be analyzed to reveal statistical descriptions in fine-scale spatial frequency ranges determined by the sonar frequency. Included in the geomorphology would be the rms heights (referred to as microroughness here) in a wavelength band just shorter than a few acoustic wavelengths and rms slopes in a band from a few acoustic wavelengths to the size of the sonar footprint. For the purposes of this work, it is assumed that all the scattering is attributed to roughness at the water/sediment boundary. We propose to use the information content in the backscattering strength versus incident angle curve to extract this information. Extracting these parameters requires a valid scattering model that incorporates them. Ideally, this model would be simple enough to use in real-time as a bathymetric survey progresses.

Two approaches to modeling swath bathymetry and sidescan sonar image returns have been developed by the Naval Research Laboratory. Both models are fully three-dimensional and are based on Helmholtz/Kirchhoff (H/K) theory for near-normal incidence (>45° grazing). One is a fundamental approach involving the H/K integral over the scattering footprint and is suitable for Monte Carlo simulations [1,2]. (Within the current context, this model is referred to as the benchmark or groundtruth model.) The other is designed for more practical use involving a high-frequency approximation to the H/K integral, thereby simplifying it and allowing it to be used for prediction or inversion [3]. The latter model is referred to as BISSM (Bistatic Scattering Strength Model). In its development composite-roughness theory (originating with refs. [4,5]) is invoked. (Composite-roughness theory (CRT) is discussed further later and references more pertinent to that discussion are given.)

BISSM has been used for inversion in neural networks to test its sensitivities in the estimation of geomorphic parameters [6,7]. Lacking properly calibrated and groundtruthed data, BISSM itself

was used in that work to generate the test data sets. The technique proved to be reasonably good at estimating the rms slope and microroughness.

Still lacking real data sets, we have resorted to a revised simulation technique that is expected to have greater fidelity with real topographic scattering at high grazing angles. The approach here is to use the benchmark model to simulate scattering data for a given set of geomorphic parameters and then use the proposed prediction model to extract these parameters. This work is preliminary to the application of neural networks to invert the simulated backscatter data to recover the input geomorphic parameters. This present application of the H/K method did shed new light on the fundamental scattering process, particularly in terms of locating the split the spectrum for the application of the CRT. These new scattering results are reported here.

2. REAL AND SIMULATED GEOMORPHOLOGY

2.1 Measured Bottom Roughness Spectra

Numerous bottom spectra have been reported in the literature. References [8-11] offer some common examples, and the spectra used here are largely from those publications. Most reported spectra have followed a power law form, that is, $w(K)=aK^b$, where $w(K)$ is the amplitude spectrum as a function of the surface wavenumber (K). The spectral parameters a and b could be functions of direction on the surface, but it is assumed that the surface is isotropic and, therefore, that they are independent of direction. The surface wavenumber K is actually a dimensionless quantity so that a carries the dimensions of w(K)--this is achieved by referring K to some standard value such as, for example, 1cyc/km (cf. [8]) or 1cyc/cm (cf. [10]). A reference value 1cyc/m is chosen for this work and the values of a are modified accordingly. Moreover, it is assumed that the power law extrapolates unchanged into the wavenumber band from 2cyc/m (surface minimum wavelength of .5m) to .00782cyc/m (surface maximum wavelength of 128m). Table I gives the appropriate modified values for a for selected spectra (several spectra listed are discussed in the next two sections). To aid in interpreting the scattering plots given later, Fig. 1 illustrates the forms of the various power law spectra.

2.2 ARSRP Measured Bottom Roughness Spectra

The Office of Naval Research is conducting a program for measuring low-frequency scattering for the seafloor called the Acoustic Reverberation Special Research Program (ARSRP). A site just off the Mid-Atlantic Ridge (MAR) was selected for detailed

TABLE I: Parameters of selected spectra

SOURCE SPECTRUM	REF	SPECTRUM LABEL	a (m^3)	b	STD DEVIATIONS LS slope	σ_μ*
Caruthers& Novarini	[11]	C&N	1.86e-2	-1.75	11.8°	0.059 m
Czarnecki& Bergin	[9]	C&B	1.53e-3	-2.27	7.4°	0.006 m
Gorda Rise (shrt WL)	[8]	GORDA	2.42e-3	-1.74	0.15°	0.001 m
TuftsAbys (shrt WL)	[8]	TUFTS	1.56e-3	-1.04	0.19°	0.004 m
MissionBay	[6]	MSBAY	1.32e-7	-1.59	5.1e-5	0.000 m
Made up		surfC	6.31e-2	-1.60	23.8°	0.173 m
Made up		surfD	6.00e-3	-2.27	26.9°	0.017 m
Made up		surfE	6.00e-2	-2.00	9.60°	0.021 m

* microroughness bandpassed from the smallest wavelength to one acoustic wavelength.

reverberation work and for the measurement of very high resolution bathymetry. Later in 1993, geomorphology will be surveyed and resolved to about 1m in selected areas. Available at this time, however, is bathymetry resolved to 200m [12]. This bathymetry was used [11] to evaluate spectra for MAR region and to fit to it an isotropic power law spectrum (although spectra for the region were quite directional in long wavelengths). The resulting spectrum is labeled C&N.

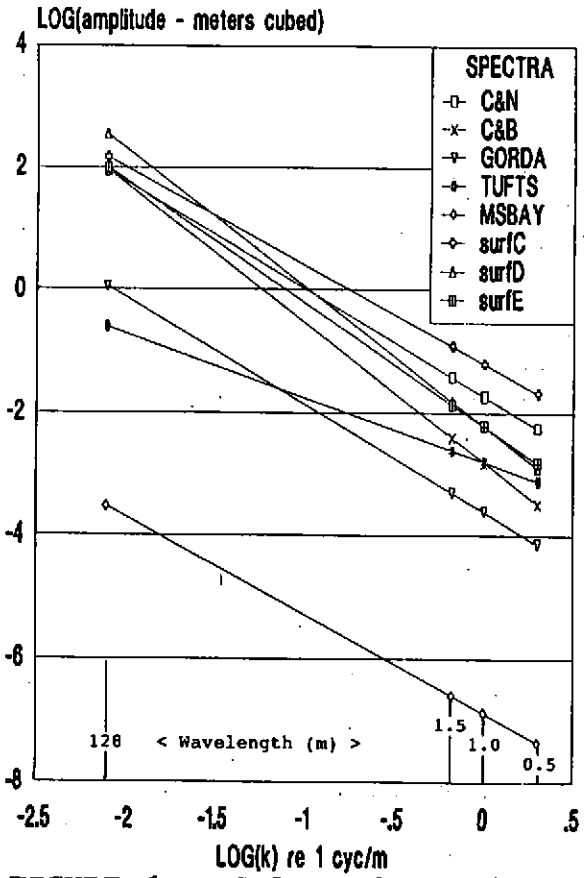

FIGURE 1: Selected amplitude spectra

2.3 Simulated Geomorphology

As will be discussed in the next section, the model is used to simulate the groundtruth scattering involves integrals over actual realizations of two-dimensional surfaces. The technique used for simulating the surfaces was originally reported in 1971 [13] and most recently reported for the simulation of the two-dimensional geomorphology in the MAR region in ref. [11]. Surface realizations are generated for all the power law spectra given in Table I. The surface size is 256m square and the grid is .25m square (1024 by 1024 points). Bathymetry with

wavelengths greater than 128m is assumed to be is deterministic and scattering controlled by slopes and strikes of facets that size or greater can be handled deterministically, and is, therefore, ignored here.

As will be seen later, there is a narrow band of seafloor wavelengths that produce useful scattering results (i.e., scattering results for which estimates of geomorphic parameters can be made) for a given acoustic frequency. Therefore, some of the scattering results are not presented here because their simulated surfaces are either too smooth or too rough. To provide additional results in the band of interest for interpretation, three spectra that fit the useful range of scattering are made up. These spectra are labeled surfC, surfD, and surfE in Table I. Essentially, they were taken from measured spectra by modifying either a or b, or both slightly.

3. SCATTERING THEORY

3.1 Helmholtz/Kirchhoff Theory

As the benchmark, the model developed by Caruthers et al. [1] consisting of evaluating numerically the full H/K integral is adopted. The model is described in ref. 1. The complex scattered field for a point source and a 2-D surface is calculated assuming a cosine squared ensonification function. Neither Fraunhoffer nor Fresnel approximation is invoked and the full wavefront curvature is kept in the calculations. The scattered intensity is then obtained as the ensemble average of pp* over an ensemble of subareas, where p is the complex scattered pressure at a point. The receiving point is selected to coincide with the source point to obtain backscattering strength. The backscattering strength is calculated from $SS=10\ \log(\langle pp^* \rangle/(A*I_i)$, where A is the ensonified area and I_i the incident intensity.

3.2 High-Frequency Limit -- BISSM

Backscattering strength can be expressed as the sum of two terms: one accounting for diffuse scattering from microroughness and the other accounting for scattering from larger scale features. The first one has been shown to be adequately represented by Lambert's law with an empirically determined coefficient, but is physically related to Bragg scatter from the microroughness. The latter term is most significant near the specular direction and represents scatter from a collection of large-scale facets. It depends on the orientations of the facets. We have modified this slightly from standard treatments (e.g., [14] pp 207) by the inclusion of small-scale roughness on the facets which affects the forward scatter direction as well as Bragg directions. Forward scatter is modified to include the Eckart factor (i.e.,

e^{-g} where g is a roughness parameter squared--essentially the microroughness scaled to the wavelength) [15]. Further details on the form of the model can be found in ref. [3]. The important issue here is locating the partition between these scales. This is often treated in the literature under the subject of composite-roughness theory, which is discussed next.

3.3 Composite-Roughness Theory

Disregarding the deterministic large scale, BISSM is a two-scale model as often treated in CRT: small-scale scattering controlled by microroughness and large-scale controlled by slope statistics. The critical question in CRT is where to partition the two scales [16-19]. There are two primary effects in locating the partition: Scattering in the near-specular direction and scattering near the transition between slope and roughness controlled scattering. McDaniel [19] showed that, if diffractive corrections are included, both effects are greatly reduced. An analysis of McDaniel's Eq. (16) reveals that the third term in the exponential is the Eckart factor within the approximations that allow it to come out of the integral. This reduces the effect of partition selection near specular. McDaniel's fourth term corrects the problem at the junction between large-scale and small-scale controlled scattering. It appears that the problem is really a difficulty with Bragg scatter calculations with only very short wavelengths present when the partition is made at a short-wavelength cutoff. To the extent that Lambert's law is a valid representation of wide-angle, small-scale scattering, this latter effect is less of a problem in our implementation of CRT in BISSM, but it is neglected here since we have no good measure for Lambert's coefficient in our case.

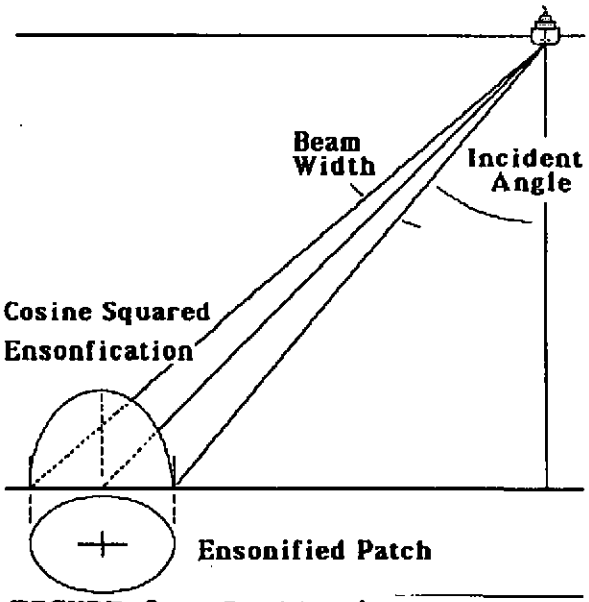

FIGURE 2: Scattering geometry

4. SIMULATING SCATTERING FOR SWATH BATHYMETRY/SIDESCAN SONARS

The geometry for scattering is designed to simulate a standard bathymetric/sidescan sonar system with a swath half-angle of 45° and beamwidth of 2°. To reduce the computational load, a relatively low frequency (for swath systems) of 1kHz is chosen.

(One simulation is made at 2kHz.) The ensonified scattering patch varies in shape and size in a natural geometric manner with variation of incident angle. Figure 2 shows the geometry for the beam at about 45°. Surfaces several times the size of the endonified patches were simulated. For scattering at any given angle, an ensemble average is taken over the number of independent patches that could fit onto the surface. This ranges from nine at normal incidence to two at 45°. Because we are using only a few realizations in the ensemble, we smooth the results over three points in angle (6 deg).

5. RESULTS AND CONCLUSIONS

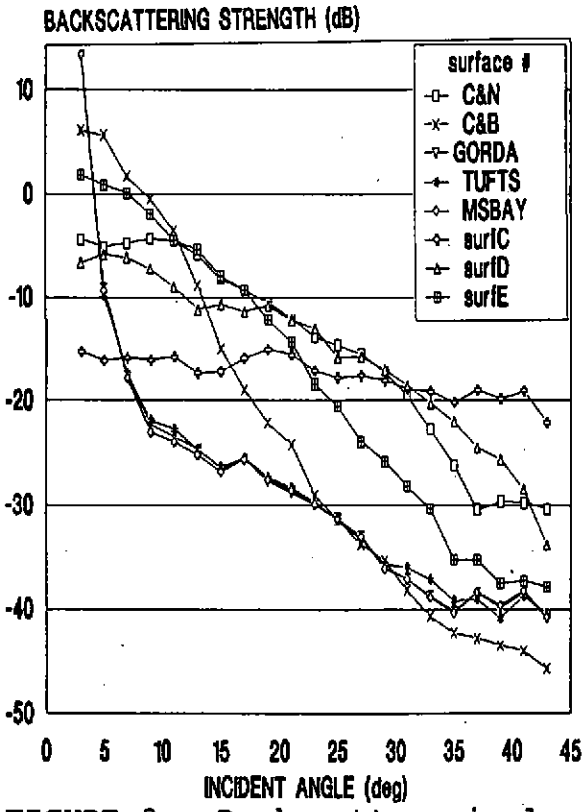

FIGURE 3: Backscatter simulation with H/K integral

as general broading and saturation at -40 dB. (This is only a matter of compromising to match a reasonable computational load.) This affects the scattering curve for incident angles in excess of 30°.

The overall results of the application of H/K model are shown in Figure 3. The smoothest surface is MSBAY which is essentially flat, but it might be noted that GORDA and TUFTS also appear to be very flat to the 1kHz sound. Additional analysis, not shown here, has indicated that for these very flat surfaces diffraction effects caused by the finite size of the ensonified patches are appearing

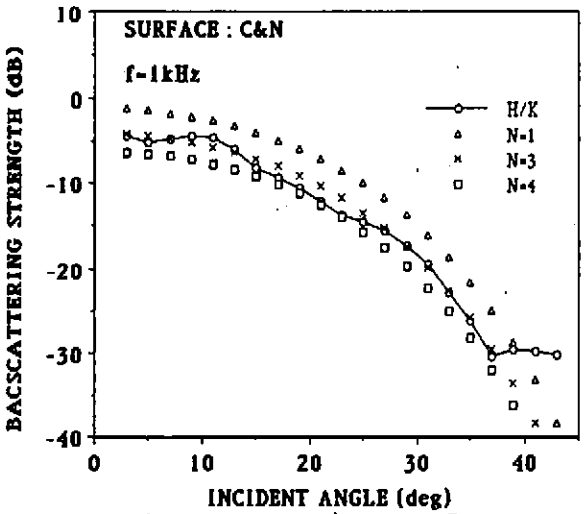

FIGURE 4: Comparison of BISSM to H/K simulation, effect of wavelength partition index N

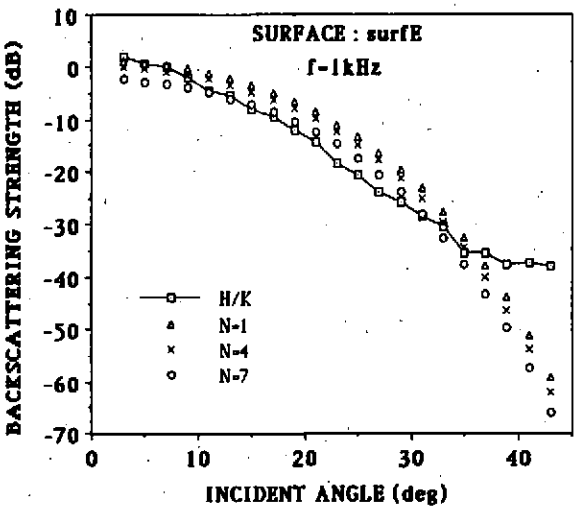

FIGURE 5: Comparison of BISSM to H/K simulation, effect of wavelength partition index N

Surfaces with slightly increased roughness (e.g., C&B) show increased scattering in the central lobe, but decreased for angles beyond 30°. This is explained by the fact that the main effect of scattering at these wide angles is to destroy the coherence of the diffraction sidelobes. Surface surfC is rougher and shows isotropic scattering with essentially no forward lobe. Surface statistics represented by these extremes define practical limits for probing with 1kHz sound. The surface whose statistics seems optimal for measurement and analysis at 1kHz is C&N.

Figure 4 shows the fit of BISSM to the benchmark model for selected values of the cutoff surface wavelength in numbers of acoustic wavelength (referred to here as the wavenumber index partition, N). Note that a reasonable fit is made at N=3. This suggests that for this case, facets the size of three wavelengths can be treated as reflecting facets and scattering is controlled by their slopes. All roughness at scales below three wavelengths is then included into microroughness and σ_u in Table I would be larger. The departure at higher angles is attributed to the onset of Bragg scattering, which we have neglected here.

Figure 5 shows the fit of BISSM to the benchmark model for selected values of the cutoff surface wavelength for surfE. Note that there is a reasonable fit for N between 4 and 7 (stays within 5dB over a 35dB range). Actually, the partition index may vary slightly with incident angle. Further analysis is required to understand this departure.

Figure 6 illustrates the effect of frequency on the relation of BISSM to the benchmark model. Note that one would not expect a

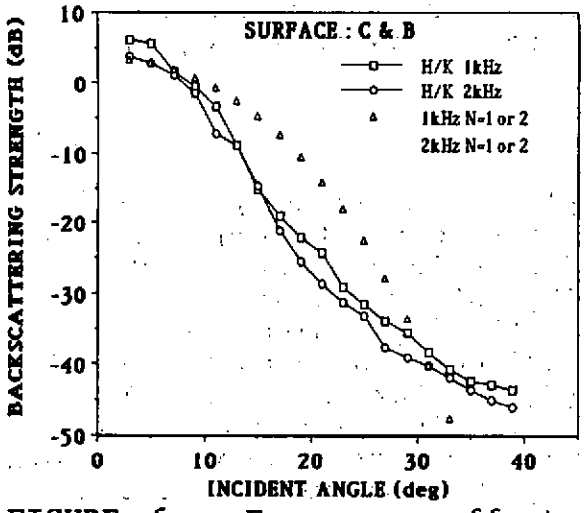

FIGURE 6: Frequency effects for wavelength partition index equal to one

frequency dependence for the slope term; however, it must be remembered that the split between CRT scales is frequency dependent and we correct the slope term with microroughness through the factor e^{-g}. Having said that, however, the BISSM results for the two frequencies show no difference. This is because this particular spectrum strongly emphasizes the low-frequency end (frequency independent slope controlled part) and e^{-g} is near unity and largely independent of changes in g. It is easily seen that there is some problem in achieving a reasonalbe fit between BISSM and H/K. It is likely that the surface is so smooth that diffraction dominates scattering beyond 15 or 20 degrees.

In conclusion, we have shown that within the present computational demands placed on the models: 1) BISSM is a good representation of the more sophisticated H/K model; 2) the partition in the two scales of CRT can be set by comparing BISSM results with those of H/K; and 3) the partition might vary from around one up to maybe five wavelengths, possibly in such a way as to make the facets large enough to maintain a microroughness on the facets nearly constant (just less than wavelength/2π, $e^{-g} < 1$). The point of this work was to determine if neural networks can be applied to the inversion of backscatter data for the extraction geomorphic parameters using a model like BISSM. We might conclude that it can but there may be another free parameter, the scale partition, whose effects need a better understanding.

6. ACKNOWLEDGEMENT

This work was supported in part by the Acoustics Reverberation Special Research Program of the Office of Naval Research.

7. REFERENCES

[1] JW Caruthers, RS Keiffer, and JC Novarini, 'Near-Field Acoustic Scattering from Simulated Two-Dimensional, Wind-Driven Sea Surfaces', J. Acoust. Soc. Am. 91 p813, (1992).
[2] JC Novarini, RS Keiffer, and JW Caruthers, 'Forward Scattering from Fetch-Limited and Swell-Contaminated Sea Surfaces', J. Acoust. Soc. Am. 92 p2099 (1992).
[3] JW Caruthers and JC Novarini, 'Modeling Bistatic Bottom scattering Strength Including a Forward Scatter Lobe', IEEE J. Oceanic Engr. accept for publication.
[4] BF Kuryanov, 'The Scattering of Sound at a Rough Surface with Two Types of Irregularity', Sov. Phys. Acoust. 8 p252 (1963).

MODELING SWATH BATHYMETRY

[5] W Bachmann, 'A Theoretical Model for the Backscattering Strength of a Composite-Roughness Sea Surface', J. Acoust. Soc. Am., 54 p712 (1973).
[6] JW Caruthers and BS Bourgeois, 'Geomorphic Parameter Estimation with Neural Networks using Bathymetry and Backscatter Data', J. Acoust. Soc, Am. 91 p2428 (1992).
[7] BS Bourgeois and JW Caruthers, 'Neural Network Parameter Estimation for a Bistatic Scattering Strength Model', Proceedings of Mastering the Oceans through Technology, (IEEE OCEANS'92 Conf.) p158, Newport, RI, (1992)
[8] CG Fox and DE Hayes, 'Quantitative Methods for Analyzing the Roughness of the Seafloor', Rev. of Geophys and Space Phys. 23 1 (1985).
[9] MF Czarnecki and JM Bergin, 'Characteristics of Two-Dimensional Spectrum of Roughness on a Seamount, Nav. Res. Lab., Rept. 9022, (1986).
[10] KB Briggs, 'Microtopographical Roughness of Shallow-Water Continental Shelves', IEEE J. Oceanic Engr., 14 p360 (1989).
[11] JW Caruthers and JC Novarini, 'Simulation of Two-Dimensional, Fine-Scale Geomorphology', J. Acoust. Soc. Am., 92 p2302 (1992).
[12] B Tucholke, bathymetric data gridded at 200m (private communications).
[13] JW Caruthers and JC Novarini, 'Numerical Modeling of Randomly Rough Surfaces with Application to Sea Surfaces', Tech. Rept. 71-13-T, Dept. of Oceanog. Texas A&M Univ. (1971).
[14] LM Brekhovskikh and YuP Lysanov, Fundamentals of Ocean Acoustics, Springer-Verlag, Berlin, 1991.
[15] C Eckart, 'The Scattering of Sound from the Sea', J. Acoust. Soc. Am., 25 p566 (1953).
[16] E Bahar, DE Barrick, and MA Fitzwater, 'Computation of Scattering Cross Sections for Composite Surfaces and the Specification of the Wavenumber where Spectral Splitting Occurs', IEEE Trans. Antennas Propag. 31 p698 (1983).
[17] ST McDaniel and AD Gorman, 'Acoustic and Radar Sea Surface Backscatter', J. Geophys. Res., 87 p4127 (1982).
[18] ST McDaniel and AD Gorman, 'An Estimation of the Composite-Roughness Scattering Model', J. Acoust. Soc. Am., 73 p1476 (1983).
[19] ST McDaniel, 'Diffractive Corrections to the High-Frequency Kirchhoff Approximation', J. Acoust. Soc. Am., 79 p952 (1986).